Botanical Studies (2008) 49: 57-66.

Vegetation deficiency in a typical region of the Loess Plateau in China

Anning SUO, Yong LIN, Jianping GE*, and Xiaojun KOU

College of Life Science, Beijing Normal University, Beijing 100875, P.R. China

(Received February 21, 2006; Accepted August 6, 2007)

ABSTRACT. Located in the central Chinese Loess Plateau, the Jinghe River is one of the major tributaries of the Yellow River, and the river basin it inhabits is characterized by a continental climate. Considering that land degradation has been the main ecological problem in the Jinghe River Basin, there is an urgent need to scientifically explore the land degradation mechanism in order to restore natural ecological environments, prevent further irreversible degradation, and retain value of these productive lands. To that end, a potential vegetation prediction and current vegetation degradation evaluation of the study area are the first and foremost jobs worth doing. In this paper, the Holdrige method is used to calculate the annual Aridity Index (AI), and a climate-vegetation based AI-NDVI model was proposed to predict the potential vegetation index, on which basis the potential vegetation index and potential vegetation distribution were both obtained. With the potential vegetation index and current vegetation index, the gap between the current and the potential vegetation was easy to calculate. This gap exhibits vegetation degradation objectively in the Jinghe River Basin. The AI-NDVI approach is expected to prove effective for ecological planning and management on a landscape and regional scale and to fuel integration between hydrology and ecology during ecological restoration research.

Keywords: Ecological restoration; Potential vegetation; The Loess Plateau; Vegetation deficient index.

INTRODUCTION

As an important component of the terrestrial ecosystem, vegetation has long been a research focus for ecologists and botanists. The role of vegetation in soil and water conservation on the Loess Plateau has been well documented (Chen and Wan, 2002). However, how seriously the current vegetation has been degraded and how far it is from its original state are hotly debated. According to geobotany and historic geography, human activities are responsible for the degradation of the original vegetation in the Loess Plateau and have led to a big gap between the current vegetation and the original vegetation (Wu, 1980; Zhu, 1983; Shi, 1991). Physical geographists and quaternary environmentalists have argued that the gap between the current vegetation and the original vegetation is not as big as some have asserted, and that the Loess Plateau was not within the typical forest distribution region from the perspective of climate and geological history (Zhang, 1992; Liu et al., 1996; 2003). The original vegetation is the undisputed key to this controversial question, but this no longer exists in most of the Loess Plateau.

A number of small-scale local studies of the vegetation degradation on the Loess Plateau have been carried out (Chen and Wan, 2002), but landscape and regional scale investigations with adequate ecological details are still scarce. Such large scale studies have now become feasible largely because of the development of remote sensing and spatial information technologies (Wu and Hobbs, 2002). Remote sensing has been widely used to monitor vegetation dynamics (Bastin et al., 1995; Tong et al., 1996; Boyle et al., 1997; Tanser and Palmer, 1999; Schmidt and Karnieli, 2000). Many, if not most, of these studies, however, evaluated the conditions of vegetation degradation based only on an above-ground biomass estimated using the NDVI. Potential vegetation is defined as the maximum biomass which would be established in a given area assuming no human influence (Rey, 1999). The term potential evapotranspiration (PET) is needed to determine the hydrological balance, which in turn dictates the potential vegetation that a particular place may harbor (Woodward, 1987; Running and Coughlan, 1988; Woodward and Mckee, 1991; Prentice et al., 1992; Neilson, 1993; Prentice et al., 1993; Neilson and Marks, 1994; Neilson, 1995). Most studies to date have only focused on PET modeling and assumed that large-scale vegetation units can be characterized by the predominance of one or more PETs (Rey, 1999; Zhao, 2004; Kimura et al., 2005). None has yet taken quantitative transient responses of potent vegetation to continuing changes of PET into account.

The major objective of this study was to accomplish a more detailed regional assessment of vegetation deficiency in Jinghe River Basin—one of the most representative

*Corresponding author: E-mail: gejp@bnu.edu.cn; Fax: +086-010-58808999.

geographic areas on the Loess Plateau. Our approach was to combine remote satellite data (MODIS), climatic data, DEM data, and additional field surveys. We were also interested in developing a synoptic index of vegetation deficiency that can be used to quantify vegetation deficiency in terms of both its spatial distribution and temporal dynamics. By assessing the spatial pattern and temporal dynamics of the vegetation deficiency in the Jinghe River Basin, we intended the project to provide a useful approach for large-scale assessment and management of the vegetation resources on the Loess Plateau.

STUDY SITE AND DATA SOURCE

Study site

Located in the central part of the Chinese Loess Plateau, the Jinghe River Basin (with a total land area of 45,420 km^2) drains into the middle reach of the Yellow River (Figure 1). The terrain is undulating with elevations ranging from 800 to 2,600 m. The climate is characterized by cold, dry winters and warm, humid summers. The climatic conditions in the study area show obvious spatial variation. The mean annual air temperature is 8.8°C at the northern end of the basin and increases to 10°C at the southern end of the basin. The mean annual precipitation is more than 600 mm at the western and eastern mountain side, gradually decreasing northward to only 300 mm in the northern end. There are three special characteristics of the precipitation. First, the its inter-annual variability is as high as 35%. Second, over 60% of it falls between July and September. Third, over 40% of it falls during storms. The hilly topography and intensive precipitation allows only a small portion of the precipitation to recharge the soil water supporting plants. The major portion runs off into rivers during storms. In addition, extensive human removal of the natural vegetation and farming-induced

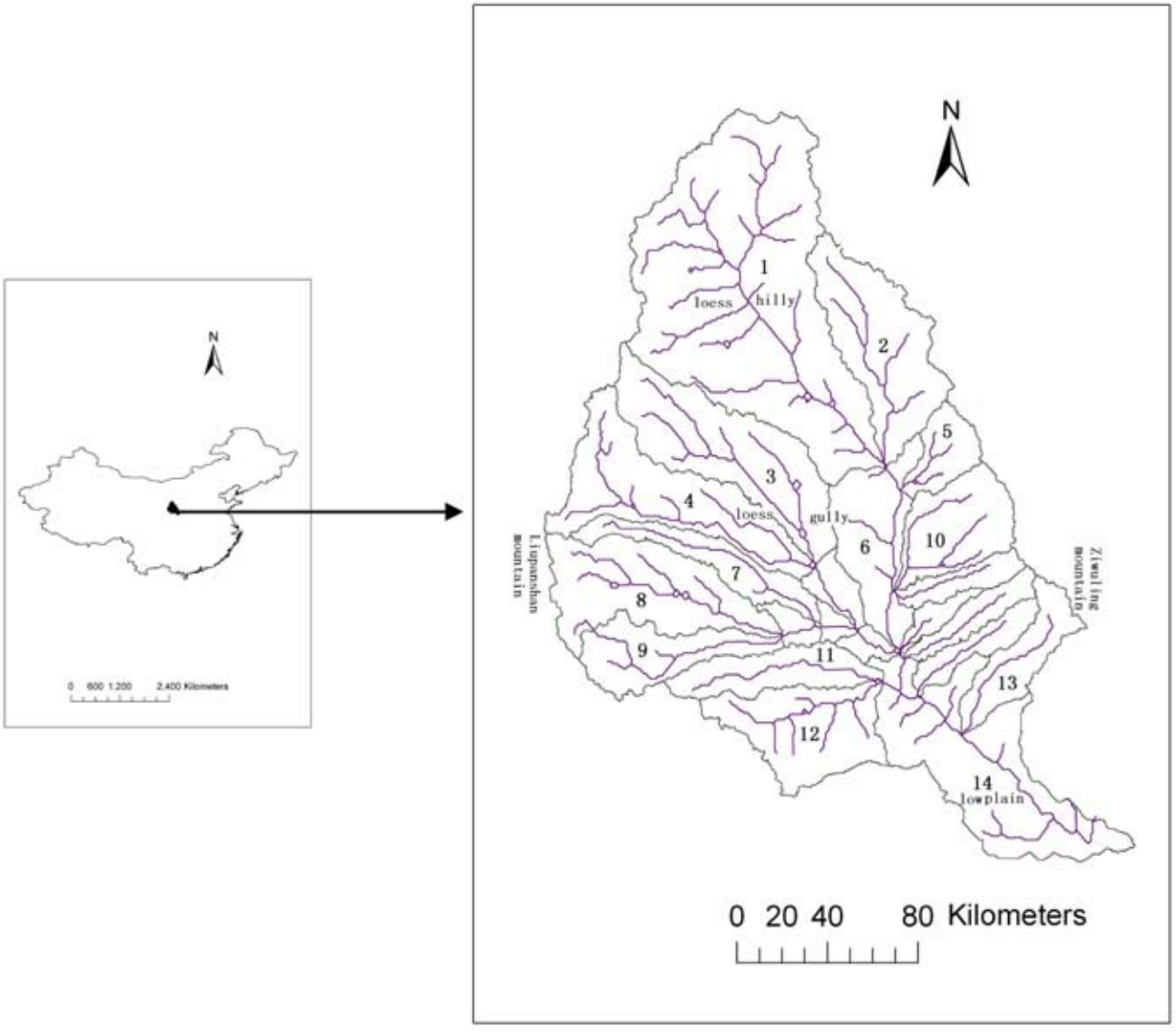

Figure 1. The location of Jinghe River Basin. Note: 1, Huajia; 2, Dongchuan; 3, Puhe; 4, Ruhe; 5, Heshui; 6, Dongzhi; 7, Honghe; 8, Upperinghe; 9, Ruihe; 10, Chengguhe; 11, Heihe; 12, Daxihe; 13, Sanshuihe; 14, Lowjinghe.

hydrological deterioration of the surface soil further exacerbates the hydrological condition of Jinghe River Basin. Thus, that the area studied contributes a solid load to the Yellow River ten times above expectations should be no surprise.

The basin has a long history of agricultural development. Most river valleys and loess gullies in the basin have been extensively cultivated, and only a small amount of secondary vegetation remains at the gully bottoms and on the ridges. More than 1320 plant species belonging to 597 genera and 128 families inhabit the basin, and these include Bryophyta, Pteridophyta, Gymnospermae and Angiosperm. Herbaceous plants and trees account for more than 900 and 400 of these species, respectively. The dominant families are Fagaceae, Betulaceae, Salicaceae, Rosaceae, Pinaceae, Poaceae, Asteraceae. On the horizontal zone from the south basin to the north basin, sparse forests mixed with arid shrublands (composed of *Ulmus pumila, Sophora japonica, Malus baccata),* arid shrublands (dominated by *Ziziphus jujuba* var. *spinosa*, *Vitex negundovar. heterophylla, Sophora viciifolia* and *Bothriochloa ischaemum*), grasslands (with *Leymus paboanus, Poa annua* and *Roegneria nutans* as constructing species) and desert grasslands (composed mainly of *Stipa bungeana* and *Stipa breviflora*) are distributed in order. In the mountainous parts of Liupanshan and Zhiwuling, arid shrublands (mainly composed of *Ostryopsis davidiana, Spiraea pubescens, Spiraea trilobata* and *Hippophae rhamnoides*) and broad-leaf forests of *Populus davidiana, Betula platyphylla,* and *Quercus liaotungensis* are distributed in vertical order from bottom to top (Chen and Wan, 2002).

Data sources

Remote sensed data (spanning from 2001 January to 2004 December) used in this study are a MODIS 32-day product at 500 m resolution provided by the Global Land Cover Facility (GLCF). For the convenience of analysis, the date has changed from the Julian day to a calendar day in advance.

Monthly average temperatures from 30 stations and precipitation from 95 rain-gauge stations in the Jinghe River Basin and its adjacent regions were provided by the China Lanzhou Arid Agriculture Climate Bureau, China's climatic bureau.

The Jinghe River topographic Map at scale of 1:250,000 is from the Institute of Geography and Resources, Chinese Academy of Sciences.

MATERIALS AND METHODS

Arid index calculation

Many studies have proved that vegetation distribution is closely related to climate (Fang and Yoda, 1990; Zeng et al., 1996; Richard and Poccard, 1998; Fu and Wen, 1999). In the Loess Plateau water availability is a decidedly limiting factor affecting plant distribution and is usually expressed by the aridity index (AI) to indicate climatic aridity. AI can be calculated by the ratio of water balance to heat balance (Wang and Xiao, 1993). Many aridity indexes have been put forth since 1990, such as the ratio of temperature to rainfall and the ratio of potential evapotranspiration (PET) to rainfall. Zhang (1993) employed the Holdrige method to plot a China PET map on the basis of 700 climatic stations with a more satisfactory vegetation-climate classification, which showed that the Holdrige method is a convenient quantitative analysis method. Other studies also found that the Holdrige method is relatively precise and agrees well with vegetation distribution (Zhou and Zhou, 1996). Therefore, the Holdrige method is used to calculate AI in this paper.

In the Holdrige method, potential evapotranspiration (PET) is calculated by an empirical formula with temperature as an input variable (Holdrige, 1947, 1976). The formula is as follows:

$$PET=58.93\times ABT \quad (1)$$

$$ABT=\Sigma t/365 \quad (2)$$

$$ABT=\Sigma T/12 \quad (3)$$

where PET is potential evapotranspiration (mm), ABT is annual bio-temperature ranging from 0 to 30°C. Daily temperatures above 30°C are set to 30°C, and those below 1°C are set to 0°C.

The ratio of PET to rainfall (P) is used to express the aridity index, and the formula is as follows:

$$K = PET/P \quad (4)$$

where K is the aridity index, and P is average annual rainfall.

Monthly climatic data from 1970 to 2003 was first processed to get the average annual rainfall for each climatic station. Then we used the DEM derived from the 1:250,000 topographic map to obtain the temperature of each station at sea level by means of a lapse rate 0.65°C/100 meter and 100×100 m grid maps of monthly temperature by way of spatial interpolation. The temperature of each cell is revised to get an actual temperature based on its corresponding elevation and the temperature lapse. The spatial distribution of potential evapotranspiration was then derived based on the temperature map.

Research showed that precipitation is closely related to longitude, latitude, and elevation (Zhao, 1988). In this paper, annual precipitation is estimated by latitude, longitude, and elevation on the basis of 1970~2003 precipitation data. The regression function is as follows:

$$P = 1297.634 - 165.413LAT + 46.822LONG + 0.0815ALT \quad (5)$$

$$R^2 = 0.769,\ a = 0.01,\ n = 32$$

with the support of GIS, a grid map of precipitation is derived based on geographic position and the corresponding elevation of the rain gauge station and

the regression function (5). Finally, we got the Holdrige aridity index distribution map of the Jinghe River Basin with the formula (4) (Figure 2).

Vegetation index calculation

The Normalized Difference Vegetation Index (NDVI) is an important monitoring index of surface vegetation features. NDVI is related to biomass, leaf area index, photosynthesis capacity, total dry mass accumulation, and net primitive yield (Birky, 2001). Therefore, NDVI is commonly used to assess vegetation cover and its dynamics monitoring on a large scale and simulate bio-physical parameters for various vegetation, land cover, and climatic change research (Fuller, 1998). NDVI can be calculated by the following formula:

$$NDVI = (\rho_{ch2}-\rho_{ch1})/(\rho_{ch2}+\rho_{ch1})\ NDVI = (-1, 1) \qquad (6)$$

where ρ_{ch1} and ρ_{ch2} are the reflection of band 1(ch1) and band 2 (ch2). Ch1 (0.58~0.68 μm) belongs to the visible band and is within the absorption band of green color, and ch2 (0.75~1.10 μm) is the infra-red band and within green plant's reflection band.

MODIS image preprocessing, NDVI computing, and false color composition were carried out with ERDAS 8.7 software to get average monthly NDVI from January to December and average summer NDVI (June, July, and August) for three years.

In this study, Jinghe River Basin on the Loess Plateau was chosen as a study region, and GIS-assisted methods were employed to estimate the spatial-temporal distribution of vegetation degradation by the following procedures. First, the Holdrige's method was used to estimate PET and calculate aridity index (AI). Second, a regression model of an aridity index (AI) and a normalized difference vegetation index (NDVI) was employed to model a potential vegetation index. Third, the vegetation deficient index expressed by the gap between potential vegetation and current vegetation was modeled spatially to show the vegetation deficient condition.

RESULTS

Relationship between aridity index and vegetation index

Spatial distribution of climatic aridity index reflects the pattern of water-heat balance (Kimura et al., 2005). In the Jinghe River Basin (Figure 2), the aridity index was the lowest (AI<0.80) on Ziwuling Mountain in the eastern basin and Liupanshan Mountain in the western basin. It ranged from 0.80 to 0.90 in southern mountain region. Because rainfall increases and temperature decreases with elevation, the water-heat balance was good in the mountain region. The aridity index in the low plain was much higher than in its neighboring loess gully regions, reflecting the important influence of local topography on regional water-heat balance. The aridity index gradually became worse with rainfall decreasing from south to north in the whole basin. The aridity index was 0.8 on the southern mountains, 1.0 in the region's center, and above 1.50 north of the basin.

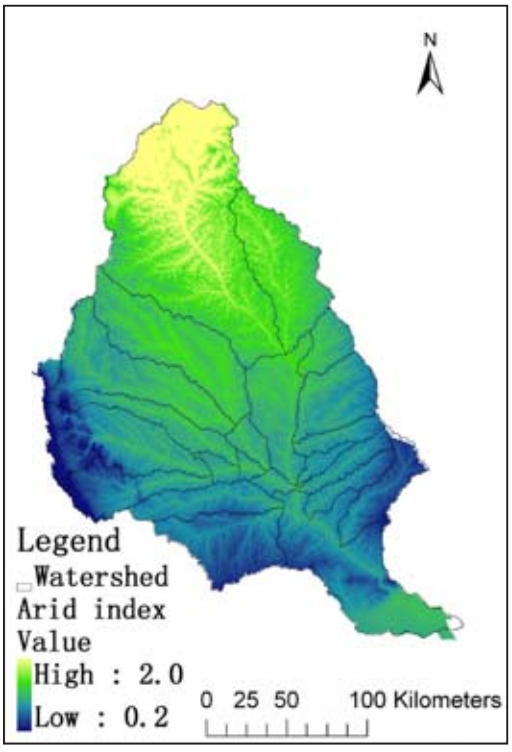

Figure 2. Aridity index spatial pattern in Jinghe River Basin.

As we all know, the distribution of natural vegetation is significantly related to the climatic aridity index. So 50 points of natural vegetation with relatively small human disturbance were selected, and their corresponding AI and NDVI values were calculated (Figure 2 and Figure 3). With these data, a scatter plot of NDVI-LAI is shown (Figure 4). It is clear that NDVI was negatively correlated with AI.

Using logic and multi-level models based on the statistical software Statistica 6.0, equations and relationships can be developed, which contain variables and their appropriate weights for spatially-explicit modeling using linear regression analyses approaches. A linear regression relationship between NDVI and AI with the best significance was selected:

$$NDVI = 1.647EXP(-1.039AI) \qquad (7)$$

R squared = 1-Residual SS/Corrected SS = 0.863,
a = 0.01, n = 50

where AI is the aridity index, NDVI is the normal different vegetation index, R squared is the correlation coefficient, residual SS is the sum of squares of residual, and corrected SS is the sum of squares of corrected total, a is the significant range, and n is the sample number. This tells us that R squared equals 0.863, which is the best performance of the model and makes the model the best choice.

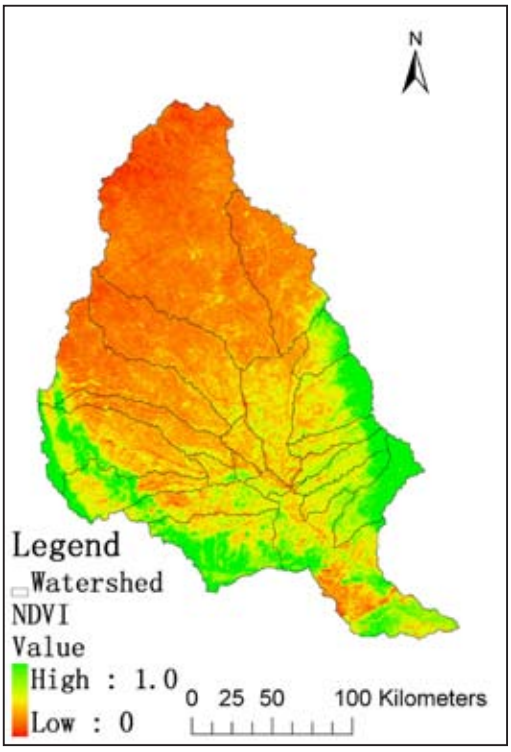

Figure 3. Vegetation index (NDVI) spatial pattern in Jinghe River Basin.

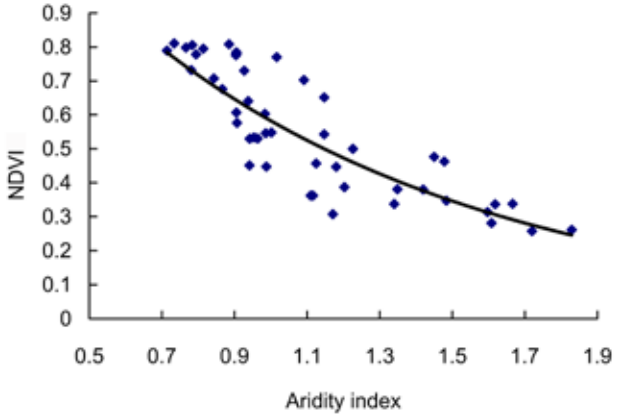

Figure 4. Relationships between vegetation index and aridity index.

Spatial pattern of potential vegetation index

The Potential Normalized Difference Vegetation Index (PNDVI) of the Jinghe River Basin is obtained based on the formula (7) with the support of Arc/info GIS. PNDVI in this basin mainly ranged from 0.50 to 0.70, which accounts for 56.15% of the basin's area, in contrast to 31.28% (PNDVI>0.70) and 12.57% (PNDVI<0.50) (Figure 5).

The spatial pattern of PNDVI varied from watershed to watershed of the basin. It was highest in the southern part of the basin and lowest in the northern part of the basin, showing a rising trend from north to south. The Daxihe watershed, in the south mountain region of the basin, boasts a 53.80% land area with PNDVI>0.80 and a 96.76% land area with PNDVI>0.70. In contrast, for the Honghe watershed, located in the basin's central part, the land area with PNDVI>0.70 only accounts for 13.7% of the watershed while land with a PNDVI ranging from 0.60 to 0.70 accounts for 81.56% area of the watershed. The PNDVI is smaller in general in the Huajia watershed in the northern basin. The PNDVI in its 52.47% land area is less than 0.50, and that in its 95.67% land area is lower than 0.60.

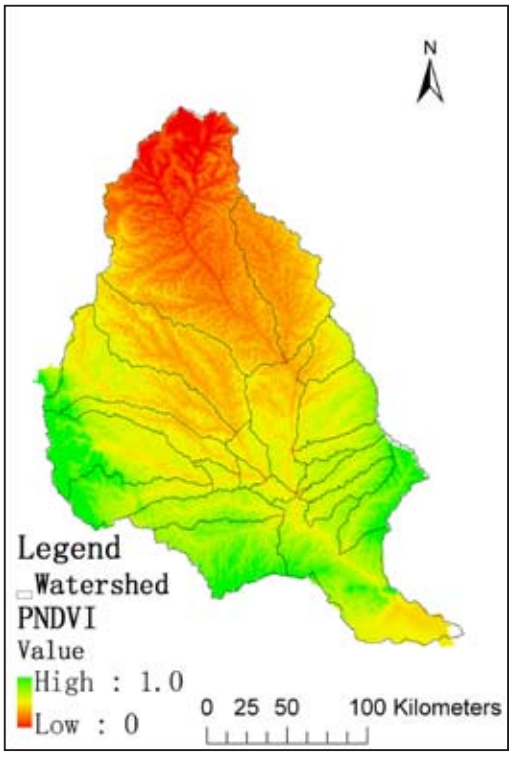

Figure 5. Potential vegetation index spatial pattern in Jinghe River Basin.

The PNDVI is higher in the mountainous regions of the western and eastern side of the basin and lower in the Yuan region of the central basin. The PNDVI in 65.39% of the Sanshuihe watershed in Ziwuling Mountain exceeds 0.80. The land with a PNDVI bigger than 0.80 in the Ruihe watershed of the west Liupanshan Mountain accounts for 42.70%. The PNDVI in the Dongzhi region on central loess Yuan and loess gully region was lower with only 3.42% of the watershed boasting a PNDVI >0.70.

Spatial pattern of potential vegetation types

Six main natural vegetation types, including warm-temperate deciduous broad-leaved forest, coniferous and broad-leaved mixed sparse forest, mesophytic shrub, dry shrub, meadow and temperate steppe, are distributed in the Jinghe River Basin according to field investigations and research reports (Chen and Wan, 2002). The potential NDVI image of the basin was classified into six natural vegetation types by a unsupervised classification approach and referred to 50 selected points (Figure 6).

As for the whole basin, the dominant vegetation types in terms of area ratio are warm-temperate deciduous broad-leaved forests (31.28%), coniferous and broad-leaved mixed sparse forests (32.44%), and mesophytic shrubs (23.71%). Warm-temperate deciduous broad-leaved forests are mainly composed of *Populus davidiana*, *Betula platyphylla, Quercus liaotungensis* et al., and mainly distributed on Ziwuling mountain in the eastern basin, Liupanshan Mountain in the western basin and southern mountain of the basin. Coniferous and broad-leaved mixed sparse forests with *Betula platyphylla suk, Ulmus pumila, Sophoro japonica,* and *Malus baccata* as constructed tree species are located in the watersheds of Honghe, Ruhe, low reaches of the Jinghe, Ruihe, Guchenghe watersheds and the Dongzhi region in the central basin. *Ostryopsis davidiana*, *Spiraea pubescens, S. trilobata* and other mesophytic shrubs are mainly distributed in loess hilly regions of Puhe, Dongchuan, and the low reaches of Huajia. In addition, arid mixed shrubs of *Ziziphus jujuba Mill.* var. *spinosa, Vitex negundo* var. *heterophylla,* and *Sophora davidii* exist in the valley and loess hilly middle regions of Huajia. Temperate steppe of *Leymus paboanus*, *Poa annua*, *Roegneria nutans*, congregated in the upper reaches of Huajia in the northern most sections of the basin. In all, 87.43% of the mountain and loess gully region in middle and south of the basin with potential vegetation was forest and shrub, and only 12.57% of the northern basin was a steppe potential distribution region.

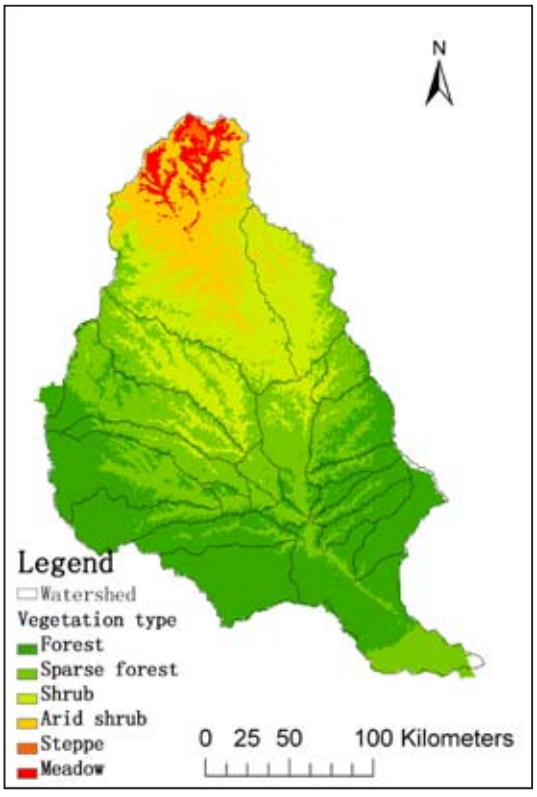

Figure 6. Potential vegetation spatial pattern in Jinghe River Basin.

Spatial pattern of vegetation deficiency

We defined the Vegetation Deficient Index (VDI) as the gap between current vegetation index (NDVI) and potential vegetation index (PNDVI). The spatial pattern of the VDI is displayed in Figure 7. Vegetation in the Jinghe River Basin was seriously damaged, which is indicated from the fact that 96.30% area of the whole basin had vegetation of different degrees of deficiency. Vegetation, in the rank of most deficiencies (VDI<-0.40), is noted as very serious (-0.40 ~ -0.30) or serious (-0.30 ~ -0.20), accounting for 2.05%, 13.97%, and 35.70% of the whole basin area, respectively. In addition, 44.55% of the basin (34.15% with VDI ranging from -0.20 to -0.10 and 10.40% with VDI at range of -0.10~0) has a slightly deficient status.

Vegetation deficiency is affected by topography, climate, human activity, and other factors. Vegetation of an extremely deficient status is mainly distributed in watersheds of Ruhe and Honghe in the loess gully region northwest of the basin, which can be seen from the following figures: VDI<-0.30 (29.85%), VDI<-0.20 (87.64%) in the Honghe watershed, VDI < -0.30 (61.20%) and VDI<-0.20 (91.33%) in the Ruhe watershed. Vegetation in the Ziwuling Mountain region in the eastern basin was slightly deficient. 29.24% of the Heshui watershed area on Ziwuling Mountain had no vegetation deficiency, and 26.66% was only slightly deficient. 56.40% of the Sanshuihe watershed area on Ziwuling Mountain had a VDI of more than -0.10, and 30.11% had

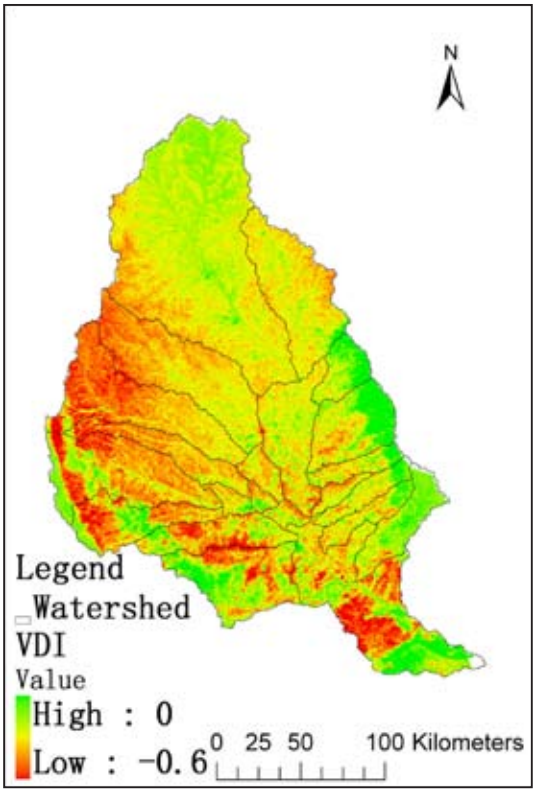

Figure 7. Vegetation deficient index (VDI) spatial pattern in Jinghe River Basin.

a VDI ranging between -0.20 ~ -0.10. Because human disturbance in the Huajia watershed in the northern basin is slight thanks to its arid climate, complex topography, and small population, the vegetation in this watershed is not as seriously deficient as we had thought. 59.72% of the watershed had a VDI ranging from -0.20 to -0.10, and 31.22% ranged from -0.30 to -0.20. Due to its flat topography and dense population, most of the land in Jingheganliu is cultivated for farming and other land usage, so vegetation deficiency in this region is much more serious than other watersheds. 7.22% of the region is with the most serious vegetation deficieny, and 19.33% of the area had a very serious vegetation deficiency, and 24.14% had a serious vegetation deficiency.

Temporal pattern of vegetation degeneration

Typical points of the six main land cover types in the basin were selected to obtain a current NDVI value and their corresponding potential NDVI. We then picked out potential NDVI dynamics of different land cover types from current NDVI series with points that their average summer NDVI value equal to PNDVI value and made vegetation deficient dynamics in a year (Figure 8). The NDVI of forests coincides very well with its PNDVI, and its VDI dynamics always varied near 0 in a time series with no vegetation deficiency. The vegetation deficiency of shrublands was small fron January to spring, and it increased from May, peaking (VDI=-0.20) in June, and varied in the range of -0.20 ~ -0.15 later. Deficiency of meadow and pasture (gaps between their current NDVI and PNDVI) was big throughout the year, especially, from June to September. Its VDI was -0.17 in July, -0.25 in August, and -0.28 in September. VDI of pasture was -0.22 in June, -0.17 in July, -0.21 in August and -0.25 in September. Crops are one of the main manmade land covers, and its vegetation deficiency showed significant human disturbance. The VDI was near 0 from January to spring. It decreased to -0.24 in May, 0.43 in June, 0.51 in July and 0.42 in August, with winter wheat ripening in May and being harvested in June and the crop land resting in July and August. The next year winter wheat is planted and germinated in September and developed in October, so its VDI increased to -0.39 in September and -0.08 in October. Desert grasslands were one of the main land cover types in the northern part of the basin. Its current NDVI was only 0.30, and its VDI was -0.18 compared to its PNDVI in the summer, which stayed more than -0.15 in later months.

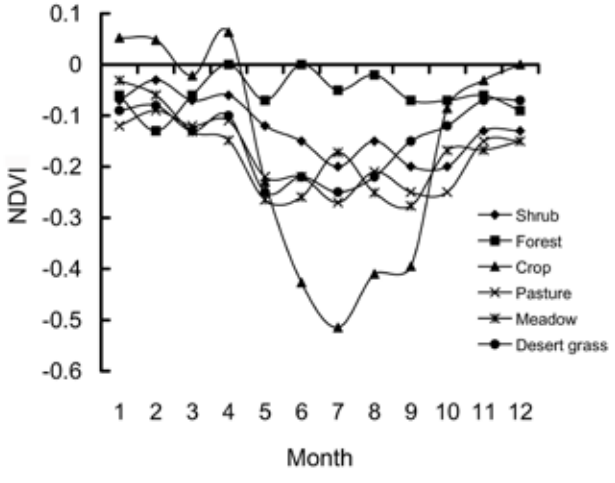

Figure 8. Dynamic of vegetation deficient index in a year.

DISCUSSION AND CONCLUSION

Evaluating a vegetation deficient condition objectively is difficult because no objective vegetation evaluation criterion exists. Many researchers have suggested using natural vegetation, original vegetation, or potential vegetation to evaluate a vegetation degeneration situation (Hou, 1983; Prentice et al., 1992; Yu et al., 2000; Sun and Chen, 1991; Ren, 2004). However, natural vegetation has only existed locally and sporadically on the Loess Plateau for hundreds of years' cultivation in most places. The original vegetation does not exist at all. Paleoecological reconstruction is a main approach in original vegetation studies. One problem is that the creation of a detailed original vegetation distribution criterion using point paleoecological remnants is difficult. Potential vegetation was a credible criterion in vegetation evaluation and ecological rebuilding. However, there is still no systematic study on potential vegetation and no referent potential vegetation map on the Loess Plateau (Fang, 2001; Li et al., 1998). The gap between current vegetation and potential vegetation is a very important research topic in ecological planning and restoration on the Loess Plateau. It could tell us how serious the current vegetation has been degraded. Therefore, potential vegetation is an ideal vegetation background in degraded vegetation evaluation.

In this paper, we first simulated the potential vegetation distribution in the Jinghe River Basin. Then, we evaluated spatio-temporal pattern of vegetation deficiency. The results showed: (1) the normalized difference vegetation index (NDVI) is closely related to the climatic aridity index (AI), and their regression model was NDVI = 1.647EXP (-1.039AI). (2) The potential vegetation in the mountainous region of the western basin, the eastern basin and most of the southern basin was warm-temperate deciduous broad-leaved forest while coniferous and broad-leaved mixed sparse forest, and mesophytic shrub were the potential vegetation in the loess gully region in the central basin. Potential vegetation in the northern part of the basin included dry shrub, meadow, and temperate steppe. In total, 87.43% of the middle-southern basin is a forest and shrub potential distribution region, and only 12.57% is a grass potential region. (3) Vegetation deficiency was high in the watersheds of Puhe, Ruhe, Honghe and lower reaches of Jinghe, Ruihe, Heihe and Jingheganliu, but very low on Ziwuling Mountain in the eastern basin, in the Daxihe watershed on the southern mountain, on the upper land of Jinghe, and on Ruihe on Liupanshan Mountain

in the western basin. It was moderate in the Loess hilly region in the northern basin. (4) In the time series, forests were not significantly deficient in all months of the one year and desert grass lands had a smaller deficiency. In contrast, the VDI for the winter wheat crop was the biggest, especially from June to September when the winter wheat was harvested in the crop land.

Experimental evidence on the potential vegetation and on the current vegetation relative deficiency is lacking. Such evidence would require a lengthy and costly investigation. However, the maps shown in Figure 5 and Figure 6 are consistent with the distribution of climate and natural vegetation of the basin, and they constitute the best possible validation of the proposed method (Vegetation Atlas of China, 2001). In spite of oversimplification of the algorithms or parameters, the method demonstrates that vegetation deficiency is markedly consistent with that surveyed. The present method may be considered to be a more useful and representative vegetation assessment, qualities which are scarce in most previous assessments (Wu and Hobbs, 2002). The method in this paper is proposed as an initial approximation to resolve the deficiencies of current vegetation assessments in most degraded vegetation regions.

Acknowledgements. This research was funded by the China National Key Foundational Research and Development Plan Program (2002CB111507) and the China National Scientific and Technical Supporting Project (2006BAD03A0206).

LITERATURE CITED

Bastin, C.N., G. Pickup, and G. Pearce. 1995. Utility of AVHRR data for land degradation assessment: a case study. Int. J. Remote Sens. **16:** 651-672.

Birky, A.K. 2001. NDVI and a simply model of deciduous forest seasonal dynamics. Ecol. Model. **143:** 43-58.

Boyle, C.A., L. Lavkulich, H. Shreier, and E. Kiss. 1997. Changes in land cover and subsequence effects on lower Freser Basin ecosystem from 1827 to 1990. Environ. Manage. **21:** 185-196.

Chen, J.M. and H.E. Wan. 2002. Vegetation Building and Water & Soil Conservation of the Loess Plateau in China. Beijing: Chinese forest Press, pp. 87-90.

Fang, J.Y. 2001. Re-discussion about the forest vegetation zonation in eastern China. Acta Bot. Sin. **43:** 522-533.

Fang, J.Y. and K. Yoda. 1990. Climate and vegetation in China. III. Water balance and distribution of vegetation. Ecol. Res. **5:** 9-23.

Fu, C.B. and G. Wen. 1999. Variation of ecosystems over East Asia in association with seasonal interannual and decadal monsoon climate variability. Climate Change **43:** 477-494.

Fuller, D.O. 1998. Foliar phenology of savanna vegetation in south-center Africa and its relevance related to climate change, PhD Dissertation, University of Maryland, College Park, Maryland.

Holdrige, L.R. 1947. Determination of world plant formation from simple climate data. Science **105:** 367-368.

Holdrige, L.R. 1976. Life Zone Ecology. San Jose, Costa Rica: Tropical Science Center.

Hou, X.Y. 1983. Vegetation of China with reference to its geographical distribution. Ann. Missouri Bot. Gard. **70:** 509-549.

Kimura, R., Y. Liu, N. Takayama, X. Zhang, M. Kamichika, and N. Matsuoka. 2005. Heat and water balance the bare soil surface and the potential distribution of vegetation in the Loess Plateau, China. J. Arid Environ. **63:** 439-457.

Li, D.Q., C.Y. Sun, and X.S. Zhang. 1998. Distribution and modeling of potential vegetation productivity in China. Acta Bot. Sin. **40:** 560-566.

Liu, H., T. Liu, and Z. Guo. 2003. Natural Vegetation of Geographical and Historical periods in the The Loess Plateau. Chinese Sci. Bull. **48:** 411-416.

Liu, T.S., Z.T. Guo, N.Q. Wu, and H.Y. Lu. 1996. Prehistoric vegetation on the The Loess Plateau: steppe or forest? J. South. Asian Earth Sci. **13:** 341-346.

Neilson, R.P. 1993. Vegetation redistribution: a possible biosphere source of CO_2 during climatic change. Water Air Soil Pollute **70:** 659-673.

Neilson, R.P. 1995. A model for predicting continental- scale vegetation distribution and water balance. Ecol. Appl. **5:** 362-385.

Neilson, R.P. and D. Marks. 1994. A global perspective of regional vegetation and hydrologic sensitivities from climatic change. J. Veg. Sci. **5:** 715-730.

Prentice, I.C., T.S. Martin, and W. Cramer. 1993. A simulation model for the transient effects of climate change on forest landscapes. Ecol. Model. **65:** 51-70.

Prentice, I.C., W. Cramer, S.P. Harrison, R. Leemans, R.A. Monserud, and A.M. Solomon. 1992. A global biome model based on plant physiology and dominance, soil properties and climate. J. Biogeogr. **19:** 117-134.

Ren, G.Y. 2004. On baseline vegetation in northern China. Acta Ecol. Sin. **24:** 1287-1293.

Rey, J.M. 1999. Modelling potential evapotranspiration of potential vegetation. Ecol. Model. **12:** 3141-3159.

Richard, Y. and I. Poccard. 1998. A statistical study of NDVI sensitivity to seasonal and interannual rainfall variations in southern Africa. Int. J. Remote Sens. **19:** 2907-2920.

Running, S.W. and J.C. Coughlan. 1988. A general model of forest ecosystem process for regional application. I. Hydrologic balance. Canopy gas exchange and primary production processes. Ecol. Model. **42:** 125-154.

Schmidt, H. and A. Karnieli. 2000. Remote sensing of seasonal variability of vegetation in a semi-arid environment. J. Arid Eviron. **45:** 43-59.

Shi, N. 1991. On distribution and change of historical forest of China. Chinese Historical Geography **3:** 43-73.

Sun, X.J. and Y.S. Chen. 1991. Palynological records of Holocene Megathemal in China. Quaternary Science Rev. **10:** 537-544.

Tanser, F.C. and A.R. Palmer. 1999. The application of a remotely sensed diversity index to monitor degradation pattern in a semi-arid, heterogeneous, South African landscape. J. Arid Environ. **43:** 477-484.

Tong, C., S. Yong, and W. Yong. 1996. Remote sensing analysis of the accumulated snow disasters in the temperate rangeland. Acta Scientiarum Naturalium Uniersitatis Neimonggo **27:** 532-537.

Vegetation Atlas of China. 2001. Compiled by editorial board, Chinese Academy of Sciences; Editors in chief: X.-Y. Hou Beijing: Science Press.

Wang, Y.F. and X.M. Xiao. 1993. Climatic gradiant of main vegetation types in the The Loess Plateau region. Acta Bot. Sin. **35:** 291-299.

Woodward, F.I. 1987. Climate and Plant Distribution. Cambridge University Press, London.

Woodward, F.Y. and I.F. Mckee. 1991. Vegetaion and climate. Environ. Int. **17:** 535-546.

Wu, J. and R. Hobbs. 2002. Key issues and research priorities in landscape ecology: an idiosyncratic synthesis. Landscape Ecol. **17:** 355-365.

Wu, Z.Y. 1980. China Vegetation. Beijing: Chinese Science Press, pp. 749-1037.

Yu, G., X. Chen, J. Ni, R. Cheddadi, J. Guiot, H. Han, S.P. Harrison, C. Huang, M. Ke, Z. Kong, S. Li, W. Li, P. Liew, G. Liu, J. Liu, Q. Liu, K.-B. Liu, I.C. Prentice, W. Qui, G. Ren, C. Song, S. Sugita, X. Sun, L. Tang, E. Van Campo, Y. Xia, Q. Xu, S. Yan, X. Yang, J. Zhao, and Z. Zheng. 2000. Palaeovegetation of China: a pollen data-based synthesis for the mid-Holocene and last glacial maximum. J. Biogeogr. **27:** 635-664.

Zeng, N., R.E. Dickinson, and X.B. Zeng. 1996. Climate impact of Amazon deforestation—a mechanistic model study. J. Clim. **9:** 859-883.

Zhang, L.S. 1992. Formation, evolution and regional difference of China's physical geography. *In* M. Ren and H. Bao (eds.), Physical regions of China and the exploitation and management Beijing: China Science Press, Vol. 25, pp. 36-69.

Zhang, X.S. 1993. A classification system of vegetation-climate for global change research. Quaternary Sci. **28:** 157-167.

Zhao, S.Q., H.N. Sun, R.J. Huang et al. 1988. Modern physical geography. Beijing: Chinese Science Press, pp. 156-169.

Zhou, J.J. and L.H. Zhou. 1996. Analysis of vegetaion- climate relations in Chaidamu region by Thornthwaite and Holdrige potential evaporation index. Arid Region Res. **13:** 46-51.

Zhao, C.Y., Z.R. Nan, and Z.D. Feng. 2004. GIS-assisted spatially distributed modeling of the potential evapotranspiration in semi-arid climate of the Chinese Loess Plateau. J. Arid Environ. **58:** 387-403.

Zhu, Z.C. 1983. Distribution of forest and stepped on the The Loess Plateau. Acta Phytoecol. Geographica Sin. **35:** 122-131.

中國黃土高原典型區植被缺失研究

索安寧　林　勇　葛劍平　寇曉軍

中國北京師範大學 生命科學學院

涇河流域位於黃土高原中部，是黃河的重要支流之一。流域以大陸性氣候為主，土地退化是涇河流域的一個主要生態環境問題。目前急待解決是尋求土地退化的科學機理，以便於恢復自然生態環境，防止土地進一步的退化，保持土地的多種生產功能。為此，潛在植被預測和現生植被的退化評價在研究區很值得研究。本文首先利用 Holdrige 方法計算了年平均氣候乾燥度指數，建立了基於植被-氣候關係的 AI-NDVI 模型，並用於類比潛在植被指數和構建潛在植被空間分佈格局。在具有潛在植被指數和現生植被指數的基礎上，就可以很容易地計算出潛在植被指數與現生植被指數之間的缺失，這種缺失可以客觀地反映涇河流域植被退化的時空格局。希望這種 AI-NDVI 方法能為大尺度上的生態規劃和管理提供有效的技術支援，並為生態恢復過程中的水文學和生態學複合問題的解決奠定基礎。

關鍵詞：黃土高原；潛在植被；植被缺失指數；生態恢復。